

Donald Rapp

Ice Ages and Interglacials

Measurements, Interpretation, and Models

Third Edition



 Springer

Ice Ages and Interglacials

Donald Rapp

Ice Ages and Interglacials

Measurements, Interpretation, and Models

Third Edition

 Springer

Donald Rapp
South Pasadena, CA, USA

ISBN 978-3-030-10465-8 ISBN 978-3-030-10466-5 (eBook)
<https://doi.org/10.1007/978-3-030-10466-5>

Library of Congress Control Number: 2018965882

1st edition: © Praxis Publishing Ltd, Chichester, UK 2009

2nd edition: © Springer-Verlag Berlin Heidelberg 2012

3rd edition: © Springer Nature Switzerland AG 2019

This work is subject to copyright. All rights are reserved by the Publisher, whether the whole or part of the material is concerned, specifically the rights of translation, reprinting, reuse of illustrations, recitation, broadcasting, reproduction on microfilms or in any other physical way, and transmission or information storage and retrieval, electronic adaptation, computer software, or by similar or dissimilar methodology now known or hereafter developed.

The use of general descriptive names, registered names, trademarks, service marks, etc. in this publication does not imply, even in the absence of a specific statement, that such names are exempt from the relevant protective laws and regulations and therefore free for general use.

The publisher, the authors and the editors are safe to assume that the advice and information in this book are believed to be true and accurate at the date of publication. Neither the publisher nor the authors or the editors give a warranty, express or implied, with respect to the material contained herein or for any errors or omissions that may have been made. The publisher remains neutral with regard to jurisdictional claims in published maps and institutional affiliations.

This Springer imprint is published by the registered company Springer Nature Switzerland AG
The registered company address is: Gewerbestrasse 11, 6330 Cham, Switzerland

Preface

The typical description of the past 800,000 years would be that the Earth has experienced about nine major periods of glaciation (“Ice Ages”) spaced at various intervals ranging from 0.9 my to 1.1 my (see Fig. 8.23). This presupposes that Ice Ages are unusual departures from normalcy. Actually, it appears as if the natural state of the Earth during this period was an Ice Age, but there were about nine interruptions of the glacial state, during which the Arctic climate was much warmer for time periods of the order of 10,000 years or so. Each Ice Age required many tens of thousands of years to develop to its maximum state of glaciation.

During the last glacial maximum, some 20,000 years ago, Canada and the northern USA were blanketed by huge ice sheets, up to 4 km in thickness. In addition, there was a large ice sheet covering Scandinavia that reached down into Northern Europe. The Antarctic ice sheet was somewhat more extensive than today. Local glaciations existed in mountainous regions of North America, Europe, South America and Africa, driving the tree line down by up to 700–800 m. The temperature of Greenland was lower by up to 20 °C, but the climate was probably only a few degrees colder than normal in the tropics. Conditions were very harsh 20,000 years ago at the last glacial maximum (LGM).

These ice sheets tied up so much of the Earth’s water that more than 150 m of ocean was removed. As a result, the shorelines of the continents moved outward by a considerable distance. The Beringia land bridge from Siberia to Alaska was created, allowing animals and humans to cross from one continent to the other. In the upper-mid latitudes, the climates were semi-arctic and the flora shifted to tundra. Humidity was reduced, and many lands dried out. At the LGM, the CO₂ concentration dropped below 200 ppm, and this combined with cold, led to plant starvation and desertification of marginal areas. The sharp temperature discontinuity at the edges of the ice sheets generated violent winds that swept up dust and dirt from dry regions, filling the atmosphere with dust. Dust deposited on the ice sheets preceded each termination of an Ice Age, allowing much greater solar absorption and the demise of the ice sheets. This last Ice Age began to wane around 17,000 years ago and dissipated through a series of gyrating climate oscillations, ending in a comparatively benign period that has lasted for the past ~10,000 years, called the *Holocene*.

A few geologists of the nineteenth century were perceptive enough to read the signs in the rocks and geological formations, and concluded that the Earth must have once (or more) been heavily glaciated with massive ice sheets that generated the markings and rock depositions that they observed. They eventually overcame the initial resistance to this new (and shocking) concept in the geological community. But it was not until the 1970s that extensive studies of marine sediments (followed by polar ice core studies in the 1980s and 1990s) demonstrated the existence, amplitude and recurrent chronology of multiple Ice Ages.

During the nineteenth century, several scientists proposed that Ice Ages could have resulted from semi-periodic variability in the Earth's orbital parameters, which change the relative solar energy input to higher latitudes. As the theory goes, when summer solar energy input to higher northern latitudes drops below a critical threshold range, ice and snow can better survive the summer. Data acquired in the twentieth century suggests that ice sheets slowly begin to form over many millennia at latitudes roughly in the range 60°N to 70°N. As the ice cover spreads, the albedo (reflectivity) of the region increases, further adding to the cooling effect. More and more water leaves the oceans and gets deposited into the building ice sheets, lowering the oceans and extending shorelines outward. Since land has a higher albedo than oceans, this provides further cooling. In the regions adjacent to the ice sheets, vegetation is inhibited, adding still further to increased Earth albedo. As the northerly regions cool, the concentrations of key greenhouse gases, water vapor, CO₂ and CH₄, decrease, adding to a worldwide cooling effect that makes the budding Ice Age a global phenomenon. Other effects such as widespread dust storms and expansion of sea ice and mountain glaciers also contributed. Thus, a runaway expansion of ice sheets develops over many millennia. James Croll formulated the concept of the solar trigger for Ice Ages based on variations of the Earth's orbit in 1875. In the first several decades of the twentieth century, M. Milankovitch quantified this theory by carrying out extensive calculations by hand in the pre-computer age. Nevertheless, in the absence of long-term data over many Ice Ages, the astronomical theory remained an abstract concept. Furthermore, there were no credible mechanistic models that described how changing solar energy inputs to higher latitudes led specifically to alternating Ice Ages and deglaciations.

With the advent of marine sediment data in the 1970s, it became possible to compare the astronomical theory with data over many glacial cycles. John Imbrie was a pioneer in this regard. He created the SPECMAP "stack" of ocean sediment data from several sites to reduce noise and devised models with which to compare ice sheet volume (v) to solar variations. Lacking an absolute dating methodology for the sediment data, he "tuned" the chronology of the SPECMAP to the variations in solar input to high altitudes. He also used spectral analysis to show that some of the prominent frequency components of the SPECMAP variability were in consonance with known frequencies of solar variation. From this, he concluded that the astronomical model explained much of the Ice Age record—at least for the past ~650,000 years. However, there is circular reasoning involved, and one could construe his procedure to involve curve fitting as well as physics.

It seems clear that the solar input to high latitudes is involved in setting the timing of transitions between periods of glaciation, but there is no quantitative theory that predicts a priori when these transitions take place.

As ocean sediment data was extended backward in time, it became apparent that the glacial cycles were evidently controlled by the Sun, but the details were difficult to work out. Of greatest importance was the fact that the period from about 2.7 mya to about 800 kya was characterized by relatively rapid, smaller amplitude climate cycles, whereas since about 800 kya, climate cycles have consistently increased in period and amplitude. By contrast, the astronomical theory would not have predicted any such major shift in frequency and amplitude since there is no reason to believe that solar forcing to higher latitudes changed qualitatively during this time period. However, Raymo et al. (2006) proposed an explanation for this that makes good sense. There were other problems with astronomical theory as well; at some prominent occurrences of climate change, there were no corresponding variations in solar input (e.g., 400 kya). Since the 1990s, a number of studies have attempted to resolve the differences between the data and the astronomical theory. Some of these studies had an obvious and pervasive bias in favor of the astronomical theory—in some cases seemingly an attempt to preserve the simple interpretation of the theory against all odds.

Yet despite the problems with the astronomical theory, there are several tantalizing similarities between the climate data and the historical solar record. These include the correlation of several important frequencies in spectral analyses and certain undeniable rough similarities in the timing of climate and solar records over some periods during the past several hundred thousand years.

The main problem with astronomical theory is that it is not at all clear just what the theory is! What seems to be most glaringly absent from the astronomical theory is a clear quantitative mechanism by which variations in solar input to higher latitudes produce changes in climate. The theory seems to revolve about the notion that when solar input to high northern latitudes is high, the climate tends to be interglacial, and when solar input to high northern latitudes is low, the climate tends to be glacial. The cycles prior to about 800 kya follow a period of about 41 ky. Subsequent to about 800 kya, as the Earth grew colder, the ice sheets thickened considerably and the spacing of glacial cycles more than doubled. The evidence suggests that in this later regime, the natural state of the Earth was what we call an Ice Age. Lacking any other perturbation, the energy balance of the Earth (prior to modern industrial times) favored growth of ice sheets at high northern latitudes. Starting at any arbitrary time, the ice sheets grew for several tens of thousands of years. During this period of growth of the ice sheets, the peak midsummer solar input to high latitudes oscillated with its $\sim 22,000$ -year period due to precession. Up-lobes in solar slowed down expansion of the ice sheets, and down-lobes increased the rate of expansion of the ice sheets, but the Ice Age would persist through several of these 22,000-year precessional cycles. After perhaps four precessional cycles, when the ice sheets became very extensive and the global CO₂ concentration dropped below 200 ppm, a precessional

solar up-lobe led to a rapid termination of the ice sheets. They disintegrated in a mere 5500 years or so. This led to an interglacial, which was eventually followed by gradual evolution of yet another Ice Age. Evidently, solar input to high northern latitudes is involved, because all terminations occur at up-lobes in the solar oscillation. Yet, many up-lobes during an evolving Ice Age do not produce terminations. Only for a very mature Ice Age, after perhaps four or five precessional cycles, does a solar up-lobe lead to a termination. Therefore, there must be some X-factor that is necessary to induce a rapid termination, in consonance with the up-lobe in solar input. The X-factor only occurs in a very mature Ice Age.

Ellis and Palmer (2016) noted that dust levels in ice cores reached sharp peaks in mature Ice Ages, just prior to advent of terminations. They proposed that the X-factor is dust deposited on the ice sheets, driving up solar absorption, leading to rapid disintegration of the ice sheets. The dust was generated by desertification of distant marginal regions due to CO₂ starvation and cold, and transported by winds to the ice sheets.

Terminations take place typically in about 5500 years—about half an up-lobe of solar input. An interglacial follows termination. During an interglacial, dust levels are nil and the solar precession curve is on the back half of the up-lobe. After about 5500 years of the interglacial, the solar curve turns downward. Ice begins to slowly accumulate at high latitudes. But sea level remains high until sufficient ice accumulates to reduce sea level. If the duration of an interglacial is measured in terms of when dv/dt turns positive, it might be about 5500 years. But if the duration is measured by a significant drop in sea level, it might be about 20,000 years.

It is interesting to speculate when the next Ice Age might occur in the future. Since it is theorized that deposition of dust produces terminations, the current heavy deposition of soot, ash, dirt and dust on Greenland and other northern sites insures that there will not be another Ice Age in the near future. Increased CO₂ will amplify this conclusion.

South Pasadena, USA

Donald Rapp

Contents

| | | |
|----------|---|-----------|
| 1 | History and Description of Ice Ages | 1 |
| 1.1 | Discovery of Ice Ages | 1 |
| 1.2 | Description of Ice Sheets | 7 |
| 1.3 | Vegetation During LGM. | 11 |
| 1.3.1 | LGM Climate | 11 |
| 1.3.2 | Global Flora | 14 |
| 1.3.3 | Ice Age Forests | 20 |
| 1.4 | Vegetation and Dust Generation During the LGM | 22 |
| 1.4.1 | Introduction: Effect of Low CO ₂ on Plants | 22 |
| 1.4.2 | C3 and C4 Flora Differences | 25 |
| 1.4.3 | Effects of Low CO ₂ on Tree Lines | 25 |
| 1.4.4 | Source of the LGM Dust | 30 |
| 2 | Variability of the Earth's Climate | 39 |
| 2.1 | Factors that Influence Global Climate | 39 |
| 2.2 | Stable Extremes of the Earth's Climate | 43 |
| 2.3 | Ice Ages in the Recent Geological Past | 48 |
| 3 | Ice Core Methodology | 51 |
| 3.1 | History of Ice Core Research | 51 |
| 3.2 | Dating Ice Core Data | 57 |
| 3.2.1 | Introduction. | 57 |
| 3.2.2 | Age Markers | 58 |
| 3.2.3 | Counting Layers Visually. | 59 |
| 3.2.4 | Layers Determined by Measurement | 63 |
| 3.2.5 | Ice Flow Modeling | 65 |
| 3.2.6 | Other Dating Methods | 68 |
| 3.2.7 | Synchronization of Dating of Ice Cores from Greenland and Antarctica | 69 |

| | | |
|----------|---|------------|
| 3.2.8 | GISP2 Experience | 70 |
| 3.2.9 | Tuning | 70 |
| 3.2.10 | Flimsy Logic | 71 |
| 3.3 | Processing Ice Core Data | 73 |
| 3.3.1 | Temperature Estimates from Ice Cores | 73 |
| 3.3.2 | Temperature Estimates from Borehole Models | 77 |
| 3.3.3 | Climate Variations | 80 |
| 3.3.4 | Trapped Gases | 80 |
| 4 | Ice Core Data | 83 |
| 4.1 | Greenland Ice Core Historical Temperatures | 84 |
| 4.2 | Antarctica Ice Core Historical Temperatures | 89 |
| 4.2.1 | Vostok and EPICA Data | 89 |
| 4.2.2 | Homogeneity of Antarctic Ice Cores | 89 |
| 4.3 | North-South Synchrony | 90 |
| 4.3.1 | Direct Comparison of Greenland and Antarctica Ice Core Records | 90 |
| 4.3.2 | Sudden Changes | 96 |
| 4.3.3 | Interpretation of Sudden Change in Terms of Ocean Circulation | 99 |
| 4.3.4 | Seasonal Variability of Precipitation | 101 |
| 4.4 | Data from High-Elevation Ice Cores | 101 |
| 4.5 | Carbon Dioxide | 102 |
| 4.5.1 | Measurements | 102 |
| 4.5.2 | Explanations | 105 |
| 4.6 | Dust in Ice Cores | 116 |
| 5 | Ocean Sediment Data | 119 |
| 5.1 | Introduction | 120 |
| 5.2 | Chronology | 125 |
| 5.3 | Universality of Ocean Sediment Data | 129 |
| 5.4 | Summary of Ocean Sediment Ice Volume Data | 130 |
| 5.5 | Comparison of Ocean Sediment Data with Polar Ice Core Data | 132 |
| 5.6 | Historical Sea Surface Temperatures | 135 |
| 5.7 | Ice-Rafted Debris | 136 |
| 6 | Other Data Sources | 139 |
| 6.1 | Devil's Hole | 139 |
| 6.1.1 | Devil's Hole Data | 139 |
| 6.1.2 | Comparison of Devil's Hole Data with Ocean Sediment Data | 141 |
| 6.1.3 | Devil's Hole: Global or Regional Data? | 143 |
| 6.1.4 | Comparison of Devil's Hole Data with Vostok Data | 143 |
| 6.1.5 | The Continuing Controversy | 145 |

| | | |
|----------|--|------------|
| 6.2 | Speleothems in Caves | 146 |
| 6.3 | Magnetism in Rocks and Loess | 147 |
| 6.3.1 | Magnetism in Loess | 147 |
| 6.3.2 | Rock Magnetism in Lake Sediments | 148 |
| 6.4 | Pollen Records | 148 |
| 6.5 | Physical Indicators | 150 |
| 6.5.1 | Ice Sheet Moraines | 150 |
| 6.5.2 | Coral Terraces | 151 |
| 6.5.3 | Mountain Glaciers | 151 |
| 6.6 | Red Sea Sediments | 152 |
| 7 | Overview of the Various Models for Ice Ages | 155 |
| 7.1 | Introduction | 157 |
| 7.2 | Variability of the Sun | 158 |
| 7.3 | Astronomical Theory | 158 |
| 7.4 | Volcanism | 160 |
| 7.5 | Greenhouse Gases | 164 |
| 7.6 | Role of the Oceans | 164 |
| 7.6.1 | Glacial-Interglacial Cycles: The Consensus View | 164 |
| 7.6.2 | Sudden Climate Change—The Consensus View | 168 |
| 7.6.3 | Wunsch’s Objections | 171 |
| 7.7 | Models Based on Clouds | 177 |
| 7.7.1 | Extraterrestrial Dust Accretion | 178 |
| 7.7.2 | Clouds Induced by Cosmic Rays | 178 |
| 7.7.3 | Ocean–Atmosphere Model | 182 |
| 7.8 | Models Based on the Southern Hemisphere | 183 |
| 8 | Variability of the Earth’s Orbit: Astronomical Theory | 185 |
| 8.1 | Introduction | 185 |
| 8.2 | Variability of the Earth’s Orbit | 188 |
| 8.2.1 | Variability Within the Orbital Plane | 188 |
| 8.2.2 | Variability of the Orbital Plane | 192 |
| 8.3 | Calculation of Solar Intensities | 192 |
| 8.4 | Importance of Each Orbital Parameter | 194 |
| 8.5 | Historical Solar Irradiance at Higher Latitudes | 197 |
| 8.6 | Connection Between Solar Variability and Glaciation/ Deglaciation Cycles According to Astronomical Theory | 199 |
| 8.6.1 | Models for Ice Volume | 201 |
| 8.6.2 | Review of the Imbries’ Model | 209 |
| 8.6.3 | Memory Model | 213 |
| 8.6.4 | Modification of Paillard Model | 213 |

| | | |
|-----------|---|------------|
| 8.7 | Models Based on Eccentricity or Obliquity | 220 |
| 8.7.1 | A Model Based on Eccentricity | 220 |
| 8.7.2 | The Middle-Pleistocene Transition (MPT) | 222 |
| 9 | Comparison of Astronomical Theory with Data | 227 |
| 9.1 | Ice Volume Versus Solar Input | 227 |
| 9.2 | Spectral Analysis | 237 |
| 9.2.1 | Introduction | 237 |
| 9.2.2 | Spectral Analysis of Solar and Paleoclimate Data | 241 |
| 10 | Interglacials | 249 |
| 11 | Terminations of Ice Ages | 257 |
| 11.1 | Abstract | 262 |
| 11.2 | Background | 263 |
| 11.3 | Terminations | 266 |
| 11.4 | North or South (or Both)? | 271 |
| 11.5 | Models Based on CO ₂ and the Southern Hemisphere | 276 |
| 11.6 | Climate Models for Terminations of Ice Ages | 279 |
| 11.7 | Model Based on Solar Amplitudes | 285 |
| 11.8 | Dust as the Driver for Terminations | 288 |
| 11.8.1 | Introduction | 288 |
| 11.8.2 | Antarctic Dust Data | 289 |
| 11.8.3 | Correlation of Ice Core Dust Data with Terminations | 290 |
| 11.8.4 | Dust Levels on the Ice Sheets | 296 |
| 11.8.5 | Optical Properties of Surface Deposited Dust | 303 |
| 11.8.6 | Source of the Dust | 304 |
| 11.8.7 | Ice Sheet Margins | 306 |
| 11.9 | Model Based on Solar Thresholds | 310 |
| 11.10 | The Milankovitch Model Versus the Most Likely Model | 313 |
| 11.10.1 | Criteria for a Theory | 313 |
| 11.10.2 | The “Milankovitch” Model | 314 |
| 11.10.3 | The Most Likely Model | 316 |
| 11.10.4 | Unanswered Questions | 318 |
| 12 | Status of Our Understanding | 319 |
| | References | 327 |
| | Index | 343 |

Abbreviations

| | |
|--------|--|
| AABW | Atlantic Bottom Water |
| ACP | Age control point |
| AM | Amplitude modulation |
| AMO | Atlantic meridional overturning |
| AMOC | Atlantic meridional overturning circulation |
| AMSL | Above mean sea level |
| AWS | Automated weather station |
| C&L | Chylek and Lohmann |
| CAS | Central American Seaway |
| CLIMAP | The “Climate: Long-range Investigation, Mapping, and Prediction” project |
| CRF | Cosmic ray flux |
| D-O | Dansgaard–Oeschger events |
| EAIS | East Antarctic Ice Sheet |
| ECM | Electro-conductivity measurement |
| EDC | EPICA Dome C |
| EDML | EPICA Dronning Maud Land |
| EEM | Previous interglacial period named after Dutch River |
| ENSO | El Niño–Southern Oscillation |
| EOT | Eocene–Oligocene transition |
| EPICA | European Project for Ice Coring in Antarctica |
| ERBE | Earth Radiation Budget Experiment |
| GCM | Global climate model |
| GCR | Galactic cosmic ray |
| GICC | Glacial–interglacial CO ₂ cycle |
| GISP | Greenland Ice Sheet Project |
| GRACE | Gravity Recovery and Climate Experiment |
| GRIP | Greenland Ice Core Project |
| GSLR | Global sea level rise |
| gya | Billions of years before present |
| H&A | Hargreaves and Annan |

| | |
|-------|---|
| H&W | Huybers and Wunsch (2004) |
| IPCC | Intergovernmental Panel on Climate Change |
| IR | Infrared |
| IRD | Ice rafted debris |
| kya | Thousands of years before present |
| kyr | Thousands of years |
| L&R | Lisiecki and Raymo |
| L&W | Landwehr and Winograd |
| L&W | Landwehr and Winograd (2001) |
| LGM | Last Glacial Maximum |
| LIA | Little Ice Age |
| LIG | Last interglacial |
| LLS | Laser light scattering |
| M&M | The book by Richard A. Muller and Gordon J. MacDonald: <i>Ice Ages and Astronomical Causes</i> , Praxis Publishing (2000) |
| M&W | McShane and Wyner |
| MBH | Mann, Bradley and Hughes |
| MECO | Middle Eocene climatic optimum |
| MOC | Meridional overturning circulation |
| MPR | Mid-Pleistocene revolution |
| MPT | Mid-Pleistocene transition |
| MWP | Medieval Warm Period |
| mya | Millions of years before present |
| NADW | North Atlantic Deep Water |
| NGRIP | North Greenland Ice Core Project |
| NH | Northern hemisphere |
| NHG | Northern hemisphere Glaciation |
| OLR | Outgoing long-wavelength radiation |
| PAL | Present atmospheric level |
| PCA | Principal component analysis |
| PDB | Crushed belemnite (<i>Belemnitella americana</i>) from the <i>Peedee</i> Formation (Cretaceous) in South Carolina |
| PDO | Pacific decadal oscillation |
| PETM | Paleocene–Eocene Thermal Maximum |
| PI | Pre-industrial |
| RSL | Relative sea level |
| SH | Southern hemisphere |
| SMB | Surface mass balance |
| SMOW | Standard Mean Ocean Water |
| SST | Sea surface temperature(s) |
| TIMS | Thermal ionization mass spectrometry |

| | |
|-------|--|
| TOA | Top of atmosphere |
| TSI | Total Solar Irradiance |
| UWESS | University of Washington Earth and Space Sciences Department |
| VEI | Volcanic Explosivity Index |
| W&L | Winograd and Landwehr (1993) |
| WAIS | West Antarctic Ice Sheet |
| WB | Wally Broecker |
| ya | Years ago |

List of Figures

| | | |
|-----------|--|----|
| Fig. 1.1 | Erratic stone | 3 |
| Fig. 1.2 | Scratched stone | 3 |
| Fig. 1.3 | Bubble rock, Acadia, Maine | 3 |
| Fig. 1.4 | Extent of the most recent ice age in North America | 6 |
| Fig. 1.5 | Glacial striations | 7 |
| Fig. 1.6 | Extent of the ice sheets 18,000 years ago | 8 |
| Fig. 1.7 | Extent of the ice sheets 12,000 years ago | 9 |
| Fig. 1.8 | Extent of the ice sheets 8500 years ago | 10 |
| Fig. 1.9 | Extent of the ice sheets 7500 years ago | 11 |
| Fig. 1.10 | Distribution of vegetation in North and Central America at the height of the last Ice Age | 15 |
| Fig. 1.11 | Distribution of vegetation in North and Central America today if there were no agriculture | 16 |
| Fig. 1.12 | The Wrangell-Saint Elias ice field on the Alaska-Yukon border | 17 |
| Fig. 1.13 | Beringia—the connecting link between Siberia and Alaska about 18,000 ya | 17 |
| Fig. 2.1 | Variation in carbon isotope composition of shallow marine carbonates | 47 |
| Fig. 2.2 | Global average temperature over the past three million years | 49 |
| Fig. 3.1 | Isotopic fractionation in vapor and precipitation | 53 |
| Fig. 3.2 | The sintering process as snow is converted to firn and then on to ice with bubbles of air entrapped | 54 |
| Fig. 3.3 | Examples of line scan images of ice cores from various depths | 61 |
| Fig. 3.4 | Close-up examples of line scan images | 62 |
| Fig. 3.5 | Section of the GISP2 ice core from 1837 to 1838 m deep in which annual layers are clearly visible | 63 |
| Fig. 3.6 | Section of an ice core drilled in the Kunlun Mountains of Western China | 64 |
| Fig. 3.7 | a Layering as evidenced by periodic variations in $\delta^{18}\text{O}$ (Dansgaard 2005). b Layering of $\delta^{18}\text{O}$ measurements at Station Crete, Greenland | 64 |

| | | |
|-----------|--|----|
| Fig. 3.8 | Example of a 1.2-m segment of GRIP data from about 8800 ya. . . . | 65 |
| Fig. 3.9 | Example of data and annual layer markings from visual stratigraphy during the early Holocene | 66 |
| Fig. 3.10 | Ice particle flow paths | 66 |
| Fig. 3.11 | Chronology of Antarctic ice core temperatures (Kawamura 2009) | 69 |
| Fig. 3.12 | Depth-age relationship in GISP2 | 71 |
| Fig. 3.13 | Dansgaard's correlation of $\delta^{18}\text{O}$ with temperature. The circles are South Greenland and the squares are North Greenland | 73 |
| Fig. 3.14 | Present day correlations of $\delta^{18}\text{O}$ or δD with temperature | 75 |
| Fig. 3.15 | Relation between isotopic composition of precipitation and temperature in the parts of the world where ice sheets exist | 75 |
| Fig. 3.16 | Comparison of estimated temperatures at two Greenland sites. | 76 |
| Fig. 3.17 | Filtered isotope data | 78 |
| Fig. 3.18 | Rate of accumulation increased in the Holocene | 79 |
| Fig. 3.19 | Difference between isotope ratios in summer and winter. | 80 |
| Fig. 4.1 | Greenland topographical map showing locations of several major ice core sites. Numbers are elevations in meters | 85 |
| Fig. 4.2 | GISP2 estimates of global temperatures over the past two centuries. The Medieval Warm Period and Little Ice age are evident. | 86 |
| Fig. 4.3 | Ice core estimates of global temperatures during the past 12,000 years. | 86 |
| Fig. 4.4 | Greenland temperature history from GRIP over 20,000 years (smoothed data). | 87 |
| Fig. 4.5 | GISP2 ice core results taken at Greenland summit over 40,000 years | 87 |
| Fig. 4.6 | Global temperature estimates from GISP2 ice cores over 100,000 years | 88 |
| Fig. 4.7 | Greenland temperature history from GRIP (smoothed data) over 150,000 years. Interglacial periods are shown by gray shading. | 88 |
| Fig. 4.8 | Antarctica topographical map showing locations of several major ice core sites | 90 |
| Fig. 4.9 | Vostok ice core data | 92 |
| Fig. 4.10 | Estimated temperature difference from today at EPICA-Dome C versus age | 92 |
| Fig. 4.11 | EPICA Dome C temperature data corrected for elevation changes | 93 |
| Fig. 4.12 | Comparison of Vostok and Dome C ice core data. | 93 |
| Fig. 4.13 | Comparison of the Vostok and Dome Fuji isotopic records of $\delta^{18}\text{O}$ as a function of depth (Watanabe et al. 2003). | 94 |
| Fig. 4.14 | Comparison of the Vostok and Dome Fuji isotopic records of $\delta^{18}\text{O}$ as a function of time | 94 |
| Fig. 4.15 | Comparison of Greenland and Antarctica isotope records | 95 |

| | | |
|-----------|---|-----|
| Fig. 4.16 | Isotopic and CH ₄ data from Greenland and Antarctica on the GISP2 time scale | 96 |
| Fig. 4.17 | Sudden climate change events at Greenland and Antarctica | 98 |
| Fig. 4.18 | Vostok (Antarctica) record of CO ₂ , CH ₄ and temperature (from δD) | 103 |
| Fig. 4.19 | Variation of CO ₂ concentration since the LGM. | 104 |
| Fig. 4.20 | Comparison of ice volume with CO ₂ concentration across the last termination | 105 |
| Fig. 4.21 | Variation of δ ¹⁴ C and CO ₂ concentration during past 40,000 years. | 111 |
| Fig. 4.22 | Variation of temperatures and CO ₂ since the LGM. | 112 |
| Fig. 4.23 | Variation of peak solar intensity over the past 40,000 years | 113 |
| Fig. 4.24 | Sea salt sodium flux measured from the EPICA Dronning Maud Land ice core and solar forcing | 114 |
| Fig. 4.25 | Taylor Dome record of atmospheric CO ₂ over the most recent glacial termination | 115 |
| Fig. 4.26 | Phase diagram for CO ₂ as a function of temperature and pressure. | 116 |
| Fig. 4.27 | Comparison of dust flux to pCO ₂ in ice core | 118 |
| Fig. 5.1 | Fit of a portion of the δ ¹⁸ O curve to the ice model of Lisiecki and Raymo (2005). | 128 |
| Fig. 5.2 | Assignment of stages and terminations by H&W. Stages are designated by arrows and terminations are defined by circles | 129 |
| Fig. 5.3 | Universality of oxygen isotope patterns from forams from around the world. | 130 |
| Fig. 5.4 | SPECMAP showing marine isotope stage numbers. | 131 |
| Fig. 5.5 | δ ¹⁸ O for site 806. | 131 |
| Fig. 5.6 | Isotope data from a stack of 57 records. | 133 |
| Fig. 5.7 | Comparison of variation of δ ¹⁸ O data from two sources | 134 |
| Fig. 5.8 | Comparison of ocean sediment data with Antarctica EPICA-Dome C data | 135 |
| Fig. 6.1 | Measured oxygen isotope variability at Devil's Hole. | 140 |
| Fig. 6.2 | Comparison of ages from Devil's Hole with ages from SPECMAP | 142 |
| Fig. 6.3 | Alignment of Devil's Hole transition points with Vostok transition points. | 145 |
| Fig. 6.4 | Upper panel: δ ¹⁸ O from GRIP in Greenland. Lower panel: measured susceptibility of lake sediments in France | 149 |
| Fig. 6.5 | Smoothed data on sea level based on Red Sea sediments and coral terrace data | 153 |
| Fig. 7.1 | Direct and diffuse solar irradiance measured at Mauna Loa following volcanic eruptions | 161 |
| Fig. 7.2 | Global temperature change after Toba eruption | 163 |

| | | |
|-----------|---|-----|
| Fig. 7.3 | Near-surface waters flow towards four main deep-water formation regions (yellow ovals)—in the northern North Atlantic, the Ross Sea and the Weddell Sea | 166 |
| Fig. 7.4 | Schematic of the three modes of ocean circulation that prevailed during different times of the last glacial period | 167 |
| Fig. 7.5 | Total meridional heat flux of the combined ocean/atmosphere system estimated from Earth Radiation Budget Experiment (ERBE) satellites, direct ocean measurements, and atmospheric contribution as a residual. | 174 |
| Fig. 7.6 | Comparison of Greenland temperature profile with methane profile at Vostok | 176 |
| Fig. 7.7 | Comparison of radionuclide fluxes with relative amount of ice-rafted debris over the past 12,000 years | 181 |
| Fig. 7.8 | Comparison of lower troposphere cloud cover anomaly with cosmic ray anomaly over the past two sunspot cycles. | 182 |
| Fig. 8.1 | Motion of Earth about the Sun | 189 |
| Fig. 8.2 | Variation of obliquity over the past 400,000 years | 190 |
| Fig. 8.3 | Variation of eccentricity over past 400,000 years | 190 |
| Fig. 8.4 | Variation of the longitude of perihelion over the past 400,000 years. | 191 |
| Fig. 8.5 | Variability of the tilt of the Earth's orbit plane | 193 |
| Fig. 8.6 | Variation of daily total solar irradiance with day of the solar year for several northern latitudes | 195 |
| Fig. 8.7 | Calculated peak summer solar intensity and yearly average of solar intensity at 65°N | 197 |
| Fig. 8.8 | Calculated peak summer solar intensity at 65°N at three northern latitudes over the past 400,000 years. | 198 |
| Fig. 8.9 | Relative peak summer solar intensity at 65°N over 400,000 years | 198 |
| Fig. 8.10 | Relative peak summer solar intensity at 65°N over 800,000 years | 199 |
| Fig. 8.11 | Comparison of peak summer solar intensity to a horizontal surface above the atmosphere at 65°N and 65°S over 400,000 years. | 199 |
| Fig. 8.12 | Weertman's ice sheet model | 203 |
| Fig. 8.13 | Model for solar input to high latitudes used by Paillard (1998). | 210 |
| Fig. 8.14 | Dependence of the Imbries' integration on starting values for relative ice volume. | 211 |
| Fig. 8.15 | Dependence of the Imbries' integration on parameter T | 211 |
| Fig. 8.16 | Dependence of the Imbries' integration on B | 212 |
| Fig. 8.17 | Comparison of predicted ice volume from Imbries' theory with measured ice volume. | 212 |
| Fig. 8.18 | Schematic variation of v and dv/dt versus t | 215 |
| Fig. 8.19 | Schematic representation of (dv/dt) in the transitions to and from Ice Ages. | 216 |

| | | |
|-----------|---|-----|
| Fig. 8.20 | Schematic representation of $v(t)$ in the transitions to and from Ice Ages | 217 |
| Fig. 8.21 | Comparison of the solar precession curve with sea level over the past 35,000 years | 219 |
| Fig. 8.22 | Comparison of estimates of ice volume data with mid-summer solar input to 65°N | 220 |
| Fig. 8.23 | Vostok ice core data showing the spacing between rapid terminations. | 225 |
| Fig. 9.1 | Comparison of Imbries' model with SPECMAP | 229 |
| Fig. 9.2 | Comparison of inverse solar input to 65°N with slope of SPECMAP | 231 |
| Fig. 9.3 | Comparison of inverse of solar input to 65°N with slope of HW04 over the past 800,000 years | 232 |
| Fig. 9.4 | Comparison of inverse solar input to 65°N with slope of HW04 over the past 800,000 years. | 233 |
| Fig. 9.5 | a Comparison of relative ice volume of the SPECMAP with the LR04 stack b Comparison of rate of change of ice volume (dv/dt) of the LR04 stack with a solar curve. | 235 |
| Fig. 9.6 | Spectra of sine wave and sawtooth wave with 100 ky periods | 240 |
| Fig. 9.7 | Three simple functions for spectral analysis | 240 |
| Fig. 9.8 | Frequency distribution corresponding to functions in Fig. 9.6. | 241 |
| Fig. 9.9 | Function $F(t) = \cos(1.5 t) + \cos(2.5 t)$ | 241 |
| Fig. 9.10 | Spectral distribution of frequencies corresponding to function $F(t) = \cos(1.5 t) + \cos(2.5 t)$ | 242 |
| Fig. 9.11 | A hypothetical function with quasi-periodic behavior | 242 |
| Fig. 9.12 | Frequency distribution corresponding to function in Fig. 9.10. | 243 |
| Fig. 9.13 | Spectra for solar intensity at 65°N and 65°S according to M&M | 243 |
| Fig. 9.14 | Vostok time series (M&M) | 244 |
| Fig. 9.15 | Spectrum of Vostok deuterium data according to M&M | 245 |
| Fig. 9.16 | Frequency spectra of EPICA Dome-C Antarctic ice core data (Petit et al. 1999). | 245 |
| Fig. 9.17 | Spectrum of SPECMAP according to M&M and Spectrum of Imbries' ice model. | 246 |
| Fig. 10.1 | Relative sea level over the past 800,000 years, and a possible range that defines an interglacial. | 250 |
| Fig. 10.2 | High-resolution carbon dioxide concentration record. | 252 |
| Fig. 10.3 | Relative sea level over the past 800,000 years, and rough estimates of duration of interglacials, shown by blue dashed lines | 254 |
| Fig. 11.1 | Temperature deviation in Antarctic ice core and solar input to 65°N latitude over the past 450,000 years | 259 |
| Fig. 11.2 | The idealized concept of interruptions in Ice Ages | 261 |

| | | |
|------------|--|-----|
| Fig. 11.3 | Solar input to 65°N at midsummer shown along with the termination ramps. | 264 |
| Fig. 11.4 | Empirical model for termination ramp. | 266 |
| Fig. 11.5 | Superposition of nine temperature curves around the last termination | 268 |
| Fig. 11.6 | Temperature change before and through the current interglacial | 269 |
| Fig. 11.7 | Temperature change before and through the previous interglacial. | 270 |
| Fig. 11.8 | Variation of CO ₂ concentration and dust flux through the last two terminations. | 271 |
| Fig. 11.9 | Comparison of dust deposition rate and temperature change through the last and previous terminations. | 272 |
| Fig. 11.10 | Dust, temperature and solar around the time of the last and previous terminations. | 273 |
| Fig. 11.11 | Relative solar input to 65°N and 65°S showing the two periods during which both solar inputs are increasing simultaneously. | 273 |
| Fig. 11.12 | Comparison of modeled rate of dust loading with ice volume. | 281 |
| Fig. 11.13 | Comparison of modeled dust loading with ice volume | 282 |
| Fig. 11.14 | Comparison of Antarctic ice core data with calculated solar input at 65°N over 800,000 years. | 286 |
| Fig. 11.15 | Antarctic dust concentration in ice cores as measured by the Coulter method | 290 |
| Fig. 11.16 | Antarctic dust concentration in ice cores as measured by a laser optical method. | 291 |
| Fig. 11.17 | Antarctic temperature (top). Solar intensity at 65°N on June 21 (middle). Dust loading in Antarctica ice core using the Coulter counter (bottom) | 292 |
| Fig. 11.18 | Antarctic temperature (top). Solar intensity at 65°N on June 21 (middle). Dust loading in Antarctica ice core using the laser counter (bottom) | 293 |
| Fig. 11.19 | EPICA dust levels at Greenland | 296 |
| Fig. 11.20 | Ice-margin sampling site in Kronprins Christian Land. | 307 |
| Fig. 11.21 | Photo of ablation zone at Kronprinz Christians Land | 308 |
| Fig. 11.22 | Pleistocene ice with uniform debris cover and meltwater streams | 309 |
| Fig. 11.23 | Comparison of solar curves. | 311 |
| Fig. 11.24 | Comparison of smoothed Greenland temperature with yearly solar input at noon at 65°N over the past 150,000 years | 315 |
| Fig. 11.25 | Increase in dust precedes rise in CO ₂ | 317 |

List of Tables

| | | |
|------------|--|-----|
| Table 1.1 | Reductions in temperature and CO ₂ affecting the maximum tree line in the Alps and tropics | 26 |
| Table 4.1 | Characteristics of Greenland and Antarctica ice sheets | 84 |
| Table 4.2 | Characteristics of major ice core sites at Greenland | 85 |
| Table 4.3 | Characteristics of major ice core sites at Antarctica | 91 |
| Table 4.4 | Dust fluxes in g/m ² -year estimated by Lambert et al. (2015) | 117 |
| Table 7.1 | Heating and cooling effects of clouds | 177 |
| Table 10.1 | Timing of the onset and end of interglacials of the last 800 kyr and their estimated duration according to Tzedakis (2012) | 254 |
| Table 10.2 | Timing of the onset and end of interglacials of the last 800 kyr and their estimated duration according to Varga (2015) | 255 |
| Table 11.1 | Durations required for the transition from glacial to interglacial conditions | 267 |
| Table 11.2 | Relationship of the dust spikes to the ice volume curve in the Ganopolski et al. model | 283 |
| Table 11.3 | Comparison of Antarctic ice core data with calculated yearly solar input at 65°N over 800,000 years. | 287 |
| Table 11.4 | Analysis of Fig. 11.17 based on Coulter counter | 294 |
| Table 11.5 | Analysis of Fig. 11.18 based on laser counter | 295 |
| Table 11.6 | Accumulation around the time of the LGM | 297 |



History and Description of Ice Ages

1

Abstract

The existence of past ice ages was discovered by several 19th century geologists from scratch marks on rocks, erratic boulders, moraines, and other physical observations. As early as 1920, Chamberlain provided a map of the North American and Greenland ice sheets at the last glacial maximum that remain quite accurate even today. Two massive ice sheets dominated the northern hemisphere. Nearly a quarter of the earth's surface lay under the weight of a mountain of ice. The Laurentide ice sheet is believed to have reached a height of 12,500 ft. Ice covered nearly 5 million square miles of North America. As the glaciers grew, they drew so much water that the ocean levels dropped more than 100 m. The expansion of the glaciers dramatically affected the distribution and composition of vegetation. Global flora was impacted, by both CO₂ starvation than cold. Deserts expanded and wind-blown dust became prevalent at the last glacial maximum.

1.1 Discovery of Ice Ages

The history of the discovery of the existence of ice ages is summarized nicely in the small book by Woodward (2014). Imbrie and Imbrie (1979) also described this history in their classic book. In addition, Berger (2012) also presented an excellent history.

In the early 1800s, evidence began to emerge of an unusual past. This included the presence of so-called “erratic boulders”—large rounded rocks seemingly placed in inaccessible locations by a giant hand, as well as a multitude of geological evidence of past glacier evidence. However, two factors inhibited the proper interpretation of this as evidence of past ice ages. One was the overhanging influence of the Biblical description of Noah's great flood, which suggested that a great flood might have caused such phenomena. The other was the fact that in geology, there was a debate between advocates of

slow, gradual evolution of geologic formations versus change via catastrophic events, and at that time the so-called uniformitarian held sway in geology. Other ideas included the rather fantastic notion of transport of large boulders trapped in drift ice.

The Swiss were well positioned to observe the effects of past Ice Ages in the mountains of the Alps. In the 1820s, a Swiss named Venetz showed that the glaciers of the Alps were once far larger than they were at that time. Another Swiss (Charpentier) joined with Venetz in putting forth the proposition that the valleys were once occupied by enormous glaciers, as evidenced by scratch marks on rocks, erratic boulders, moraines, and other observations. A Norwegian (Esmark) found similar evidence in the Fjords. By the early 1830s, these three field investigators had found ample proof of former large-scale glaciation. Nevertheless, the scientific establishment did not give much credence to these findings.

Yet another Swiss, Louis Agassiz, under tutelage of Venetz and Charpentier, became an enthusiast for the glacial theory, and used his high position in Swiss science to promulgate these ideas. Starting in 1840 Agassiz became the main promoter of the glacial theory. In the 1840s he worked with a Scottish geologist (Buckland) to examine the geological evidence in Scotland. As the 1840s began, the glacial theory was still regarded as speculative. It was not until the 1870s that the glacial theory became widely accepted.

In the early 1800s, evidence began to emerge of an unusual past. This included the presence of so-called “erratic boulders”—large rounded rocks seemingly placed in inaccessible locations by a giant hand, as well as a multitude of geological evidence of past glacier evidence. A few geologists of the 19th century noted the presence of large boulders with characteristic scratch marks in the Swiss Alps, as well as scratch marks on the walls of rock in mountains, and suggested that these may have been generated by huge ancient glaciers that covered the mountains. The three main sources of evidence were: (1) grooves and scratches on rocks in place, and on boulders shoved along under the ice, (2) extensive unstratified deposits known as “till” traceable to glacier action, and (3) transported material (boulders) that could only have been delivered by ice (not water).

Prior to the implementation of ice core drilling and use of ocean and lake sediments to infer historical temperatures tens or hundreds of thousands of years ago, geologists had to rely on their observations of rocks and strata for guidance. Three books written around the end of the 19th century provide good insights into what was known prior to modern techniques for estimating historical temperatures. One of these books, Geike (1894) provided Figs. 1.1 and 1.2.

“Bubble Rock” in Maine is a favorite subject for photographers (see Fig. 1.3).

According to another early book, Wright (1920) showed that rocks with scratches and striations longitudinally along their longest diameters are evidence of glacial action:

It is easy to see that the stones of all sizes, while being dragged along underneath the ice, would be held in a comparatively firm grasp as to be polished and striated and scratched in a peculiar manner. On the shores of bays and lakes and in bottoms of streams we find that the stones are polished and rounded in a symmetrical manner, but are never scratched. The mobility of water is such that the edges and corners of the stones are rubbed together by

Fig. 1.1 Erratic stone (Geike 1894)

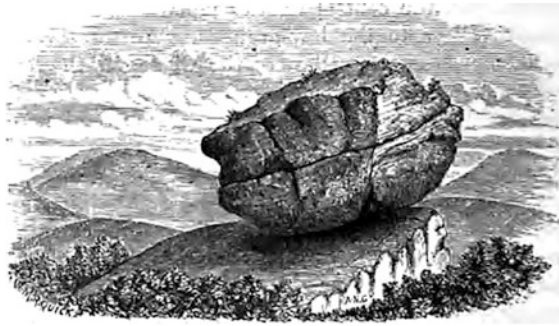


Fig. 1.2 Scratched stone (Geike 1894)

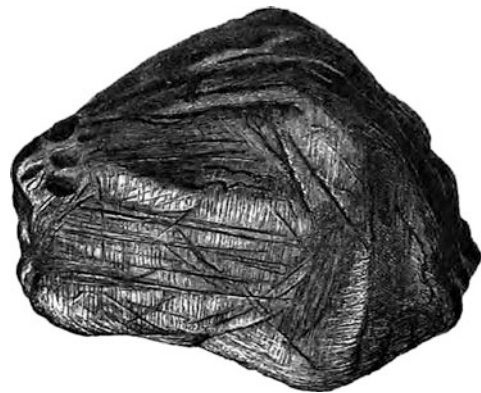


Fig. 1.3 Bubble rock, Acadia, Maine (<http://flickr.com/photos/iamtonyang/29259194/>)



forces acting successively in every possible direction. But in and under the ice the firm grasp of the stiff semi-fluid causes the stony fragments to move in a nearly uniform direction, so that they grate over the underlying rocks like a rasp From the stability of the motion of such a

substance as ice there would . . . result grooves and striation both on the rocks beneath and on the boulders and pebbles that, like iron plowshares, are forced over them. Scratched surfaces of rock and scratched stones are therefore, in ordinary cases, most trustworthy indications of glacial action. The direction of the scratches upon these glaciated boulders and pebbles is, also worthy of notice. The scratches upon the loose pebbles are mainly in the direction of their longest diameter—a result that follows from a mechanical principle, that bodies forced to move through a resisting medium most swing around so as to proceed in the line of least resistance. Hence the longest diameter of such moving bodies will tend to come in line with the direction of the motion.

However, Wright (1920) cautioned:

A scratched surface is, however, not an infallible proof of the former presence of a glacier where such a surface is found, or, indeed, of glacial action at all. A stone scratched by glacial forces may float away upon an iceberg and be deposited at a great distance from its home. Indeed, icebergs and shore-ice may produce, in limited degree, the phenomena of striation that we have just described.

Wright (1920) went on to say that although longitudinal striations can be caused by factors other than moving ice, these can be identified by the informed observer:

Stones are also striated by other agencies than moving ice. Extensive avalanches and landslides furnish conditions analogous to those of a glacier, and might in limited and favorable localities simulate its results. In those larger geological movements, also, where the crust of the earth is broken and the edges of successive strata are shoved over each other, a species of striation is produced. Occasionally this deceives the inexperienced or incautious observer. But by due pains all these resemblances may be detected and eliminated from the problem, leaving a sufficient number of unquestionable phenomena due to true glacial action.

Wright (1920) also made the point that deposits left by moving water are always stratified:

A second indubitable mark of glacial motion is found in the character of the deposit left after the retreat of the ice. Ice and water differ so much from each other in the extent of their fluidity, that there is ordinarily little danger of confusing the deposits made by them. A simple water deposit is inevitably stratified. The coarse and fine material cannot be deposited simultaneously in the same place by water alone. Along the shores of large bodies of water the deposits of solid material are arranged in successive parallel lines, the material growing finer and finer as the lines recede from the shore. The force of the waves is such in shallow water that they move pebbles of considerable size. Indeed, where the waves strike against the shore itself, vast masses of rock are often moved by the surf. But, as deeper water is reached, the force of the waves becomes less and less at the bottom, and so the transported material is correspondingly fine, until, at the depth of about seventy feet, the force of the waves is entirely lost; and beyond that line nothing will be deposited but fine mud, the particles of which are for a long while held in suspension before they settle.

In the deltas of rivers, also, the sifting power of water may be observed. Where a mountain-stream first debouches upon a plain, the force of its current is such as to move large pebbles, or boulders even, two or three feet in diameter. But, as the current is checked, the particles moved by it become smaller and smaller until in the head of the bay, or in the broad current of the river which it enters, only the finest sediment is transported. The difference

between the size of material transported by the same stream when in flood and when at low water is very great, and is the main agent in producing the familiar phenomena of stratification. During the time of a flood, vast bodies of pebbles, gravel, and sand are pushed out by the torrent over the head of the bay or delta into which it pours; while during the lower stages of water only fine material is transported to the same distance; and this is deposited as a thin film over the previous coarse deposit. Upon the repetition of the flood another layer of coarser material is spread over the surface; and so, in successive stages, is built up in all the deltas of our great rivers a series of stratified deposits. In ordinary circumstances, it is impossible that coarse and fine material should be intermingled in a water deposit without stratification. Water moving with various degrees of velocity is the most perfect sieve imaginable; so that a water deposit is of necessity stratified.

By contrast, deposits left by moving ice are not stratified:

It is evident that ice is so nearly solid that the earthy material deposited by it must be unassorted. The mud, sand, gravel, pebbles, and boulders, dragged along underneath a moving stream of ice, must be left in an unstratified condition—the coarse and the fine being indiscriminately mingled together. This is the character of the extensive deposits of loose material that cover what we designate as a glaciated region [In such an] unstratified deposit, a variety of materials is mingled that were derived from rocks both of the locality and from far-distant regions. Moreover, the pebbles in this deposit are the most of them polished and scratched after the manner of those which we know to have been subjected to glacial action.

Finally, Wright (1920) discussed the fact that the southern margin of the region where unstratified deposits containing striated stones and transported material was exceedingly irregular in two respects. The southern edge of these deposits does not follow a straight east-and-west line, but in places withdraws to the north (crenate character), and in other places extends lobe-shaped projections far to the south (serrate character). According to Wright, it was the crenate character of its southern border that was of most significance. Wright emphasized that the southern border, with its indentation, and projections was not determined by any natural barrier based on the geography of the region, but instead was determined by “the irregular losses in momentum such as would take place in a semi-fluid moving in the line of least resistance from various central points of accumulation.”

In the late 19th century, Thomas C. Chamberlain (as reported by Geike 1894) reviewed the geological evidence for glacial phenomena on the Earth’s surface, that existed prior to acquisition of ice core and benthic data on past Ice Ages. In North America, it was found that a tract of about 4,000,000 square miles had been overspread by glaciers, and nearly one-half of North America was covered with drift deposits. He mentioned concerns of the doubters but concluded: “the uncompromising evidence of the deposits themselves and by the ice-grooved rock floor on which these rest, seems to compel acceptance of the glacial theory.” Chamberlain concluded that the extent of the ice sheet was roughly as shown in Fig. 1.4. Note the three epicenters for ice sheet formation.

These descriptions represent only a fraction of the ample evidence available to late 19th century geologists that there was a previous Ice Age, although the possible existence of multiple historical Ice Ages could only be conjectured.



Fig. 1.4 Extent of the most recent ice age in North America (Geike 1894)

The University of Washington Earth and Space Sciences Department (UWESS) produced a number of excellent presentations on Ice Ages that are very descriptive and instructive. The entire structure of the great valley in Yosemite National Park is presented as an example of a classic alpine glaciated landscape.

Glacial erosion occurs by abrasion, crushing and fracturing, and quarrying of joint blocks. Ice is not hard enough to abrade rocks, but rock fragments imbedded in the base of the glacier can abrade rocky terrain below, leaving characteristic striations (see Fig. 1.5).

The UWESS described how glacier action can pluck large blocks leaving characteristic scalloped terrain. In addition, the UWESS provided many more examples and illustrations of past glacial action.



Fig. 1.5 Glacial striations (UWESS)

1.2 Description of Ice Sheets

Carroll et al. (2001) reported:

... during the late glacial period, the Wisconsin, two large ice caps, the Laurentide glacier in the East and Cordellian Glacier in the West, dominated northern North America. Nearly all of Canada lay under the two massive glaciers, which extended into the northern regions of the United States and into the southern one-third of Alaska.

These two massive ice sheets were part of an even larger system of ice that dominated the northern hemisphere. Nearly a quarter of the earth's surface lay under the weight of a mountain of ice. The Laurentide ice sheet is believed to have reached a height of 12,500 ft (Hughes 1987). Ice covered nearly 5 million square miles of North America. As the glaciers grew, they drew more than 50% of the Earth's available water, affecting precipitation The ocean levels dropped, exposing what we call the Continental Shelves. The expansion of the glaciers dramatically affected the distribution and composition of vegetation.

The leading edge of the glacier in the United States is believed to have been over a mile high (Hughes 1987). Nothing could stand in the way of this massive ice field as it pushed south, grinding over mountains and depressing the land under its massive weight. Over the ice caps, a huge high-pressure system pushed the polar jet stream southward, dominating weather patterns over much of the northern hemisphere The ice sheets influenced temperatures far to the south, and both vegetation and wildlife retreated in its front.

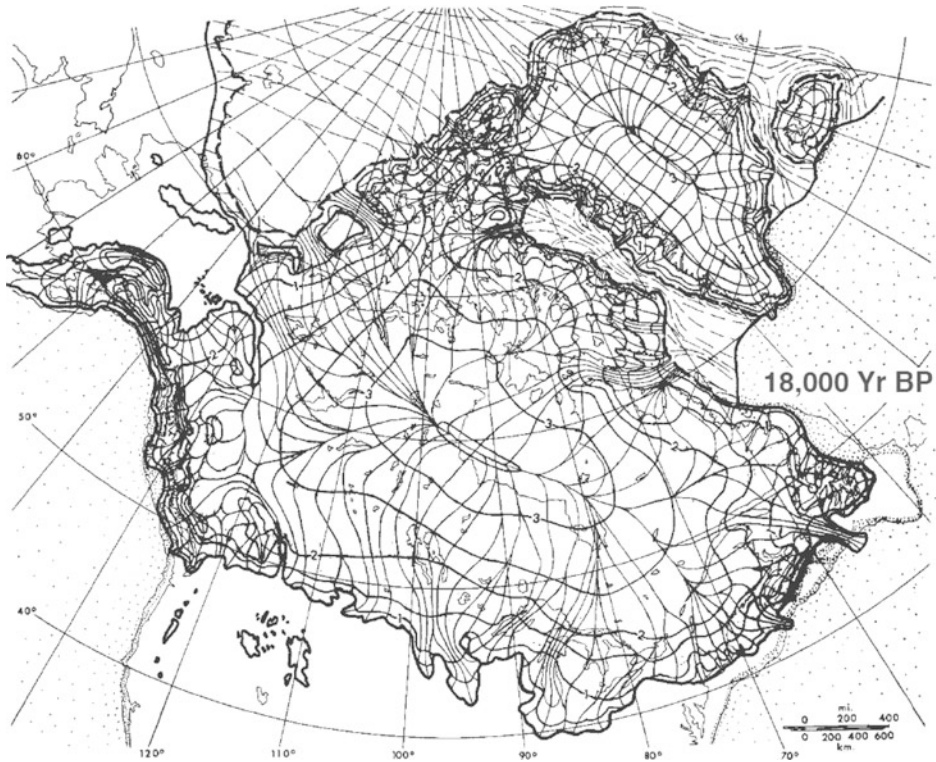


Fig. 1.6 Extent of the ice sheets 18,000 ya (Carroll et al. 2001)

Carroll et al. (2001) provided Figs. 1.6, 1.7, 1.8 and 1.9. Figure 1.6 shows the extent of the North American ice sheets at the Last Glacial Maximum (LGM). Note that the ice sheets covered all of the land above 50°N except for Alaska, and penetrated down to 40°N in the Northeastern United States. Alaska was cold enough to support ice sheets but did not receive enough precipitation. Figures 1.7, 1.8 and 1.9 show the successive depletion of the ice sheets during termination.

Hughes et al. (2015) presented a new time-slice reconstruction of the Eurasian ice sheets documenting the spatial evolution of these interconnected ice sheets every 1000 years from 25 to 10 thousand years ago (kya), and at four selected time periods back to 40 kya. At the height of the last glacial period ice sheets extended over (1) all of Greenland including the margins, out to small areas of the surrounding ocean, (2) the Barents Sea extending from Svalbard to the Kara Sea, (3) over all of Ireland and Scotland and the surrounding seas, and (4) over all of Norway, Sweden, Finland, and down to Lithuania.